The Temporal Dedifferentiation of Global Brain Signal Fluctuations During Human Brain Aging

Yifeng Wang (wyf@sicnu.edu.cn)
Institute of Brain and Psychological Sciences, Sichuan Normal University

Yujia Ao
Institute of Brain and Psychological Sciences, Sichuan Normal University

Chengxiao Yang
Institute of Brain and Psychological Sciences, Sichuan Normal University

Juan Kou
Institute of Brain and Psychological Sciences, Sichuan Normal University

Lihui Huang
Faculty of Education, Sichuan Normal University

Xiujuan Jing
Tianfu College of Southwestern University of Finance and Economics

Qian Cui
School of Public Affairs and Administration, University of Electronic Science and Technology of China

Xueli Cai
Psychological Research and Counseling Center, Southwest Jiaotong University

Jing Chen
School of Education, Chengdu Normal University

Research Article

Keywords: brain aging, fMRI, temporal dedifferentiation, global signal, lifespan.

Posted Date: August 10th, 2021

DOI: https://doi.org/10.21203/rs.3.rs-775303/v1

Abstract

The variation of brain organization as healthy aging has been discussed widely using resting-state functional magnetic resonance imaging. Previous conclusions may be misinterpreted without considering the effects of global signal (GS) on local activities and the variation of GS as age is still unknown. To fill this gap, we systematically examined the correlation between GS fluctuations and age. Correlations were evaluated between age and parameters of GS fluctuations including power at each frequency point, spectral centroids, and trends of power spectra. Data with hemodynamic response function (HRF) de-convolution and head motion parameter were further analyzed to test whether the age effect of GS fluctuations has neural origins. GS fluctuations varied as age in three ways. First, general GS power reductions were found in both time and frequency dimensions. Second, the GS power at lower frequencies transferring to higher frequencies was observed. Third, more evenly distributed power across frequencies was showed in aging brain. These trends were partly impacted by HRF de-convolution, but not by head motion. These results suggest that GS fluctuations are weaker and more evenly distributed across frequencies in elderly brain. It may indicate the temporal dedifferentiation hypothesis of brain aging from the global signal level.

1 Introduction

Resting-state functional magnetic resonance imaging (rs-fMRI) provides abundant information for large-scale brain bases of age-related cognitive changes [1]. Numerous studies have documented altered almost all functional networks with age in functional organization with rs-fMRI [1,2]. The global signal (GS) of rs-fMRI, as the average signal of the whole brain, has a great impact on the functional brain organization from local neural activities to inter-regional connections [3,4]. The characteristics of GS varying with age, therefore, is a key to understanding the age-related functional brain organization, which has not yet been elucidated.

The debate about whether the GS is signal or noise has lasted for over two decades [3]. Although early studies have found prominent artifacts (i.e. head motion, respiration) in the GS [5,6], numerous recent studies have tied GS fluctuations to vigilance [7], behavioral traits [8], brain states [9], and mental disorders [4,10], suggesting that the GS conveys particular physiological, psychological, and pathological information [11]. A recent study found a close relationship between the GS of rs-fMRI and the global EEG signal at multiple frequency bands [12]. By contrast, another study causally demonstrated that the GS could be regulated by signals from the basal forebrain [13]. Besides, Tsvetanov et al. suggested that the age effect of blood oxygen level-dependent (BOLD) signal variability could be fully explained by cardiovascular and cerebrovascular factors [14]. Since the GS has both neural and non-neural origins, it is worth exploring whether the neural and vascular factors contribute differently to the variation of GS with age.

In the current study, we aimed to investigate the age effect of GS fluctuations during the adult lifespan, using a large-sample of rs-fMRI data. Because local BOLD signal fluctuations have been reported to be

increased and decreased with age in different regions and frequencies [15,16], we expected to find frequency-dependent rise and fall of GS fluctuations with age.

2 Methods

2.1 Participants

A total of 492 volunteers (307 females, aged 19 to 80 years) were recruited from Southwest University (SWU, China) [17]. All participants reported no psychiatric disorder, substance abuse, or MRI contraindications. The project was approved by the Research Ethics Committee of the Brain Imaging Center of Southwest University, following the Declaration of Helsinki. Written informed consent was obtained from each participant.

2.2 Imaging acquisition and preprocessing

All rs-fMRI data were obtained from a 3T Siemens Trio MRI scanner (Siemens Medical, Erlangen, Germany) at the Brain Imaging Center of SWU. Subjects were asked to close their eyes, rest without thinking about any in particular, but refrain from falling asleep. Two hundred and forty-two volumes were acquired for each subject using the T2-weighted gradient echo planar imaging (EPI) sequence: 32 slices of 3 mm, slice gap = 1 mm, TR/TE = 2000/30 ms, flip angle = 90°, field of view = 220 mm × 220 mm, resulting in a voxel with 3.4 × 3.4 × 4 mm^3. The MRI data used in this study are available to the public from the International Data-sharing Initiative (http://fcon_1000.projects.nitrc.org/indi/retro/sald.html).

Image preprocessing was conducted using the Data Processing Assistant for Resting-State fMRI package (DPARSF, http://www.restfmri.net) [18] according to steps in previous studies [5,19]: removing the first 12 volumes, slice timing and realignment. Subjects whose translational and rotational displacement exceeded 2.0 mm or 2.0° or mean frame-wise displacement (FD) exceeded 0.2 were excluded. The remaining sample included 322 subjects (194 females; mean age = 41.48, SD = 17.36). Images were then normalized to the standard EPI template, resampled to a 3 × 3 × 3 mm^3 cube, and spatially smoothed (6-mm FWHM Gaussian kernel). Linear detrend, white matter, cerebrospinal fluid signals, and Friston 24 motion parameters were used as regressors to reduce head movement and non-neuronal information [20].

2.3 Power spectrum analysis of GS fluctuations

The GS was obtained by averaging signals over all gray matter voxels constrained by the binary automated anatomical labeling (AAL) 90 mask [21,22]. The Welch method with hamming window (window width 0.031 Hz, overlap rate 50 %) was applied to transform time series into frequency domain [23]. Data were cutoff within 0.007 ~ 0.25 Hz for de-noising [24]. The power-law function $y = a \times x^b$ was applied to separate the fractal trend from oscillations because the original BOLD signal consisted of a scale-free trend and multiple oscillations [25]. Frequency boundaries of oscillations were determined by the local minima on the mean power density curve of all subjects [16]. The spectral centroid (SC) of each oscillation

was calculated with Eq. (1), representing the center of gravity of the power spectrum within the given range of oscillation [26].

$$SC = \frac{\sum_{i_1}^{i_2} i \times f \times P(i)}{\sum_{i_1}^{i_2} P(i)} \quad (1)$$

Where f = 0.25/256 Hz, representing the width between two successive frequency points, $P(i)$ indicates the power at the i_{th} frequency point within $i_1 \sim i_2$ Hz.

2.4 Hemodynamic response function (HRF) de-convolution

The basic hypothesis underlying the BOLD signal is the convolution of neural events and neurovascular coupling [27]. In order to determine whether the relationship between the power of GS and age is resulted from neural activity, the blind hemodynamic response function (HRF) de-convolution approach was performed. According to our previous studies [22,28], the following steps were conducted. After noise regression, the point process analysis was adopted to detect spontaneous neural events [29]. BOLD signals larger than mean plus one SD were detected and the onsets of neural events were extracted for HRF reconstruction [30]. The HRF in each voxel was evaluated by matching BOLD signal with the canonical HRF and its time derivative. After that, neural level signals were recovered by Wiener de-convolution (http://users.ugent.be/,dmarinaz/HRF_deconvolution.html) [31].

2.5 Contributor detection for the relationship between GS fluctuations and age

The same analysis as the original data was performed for de-convolved data. The only difference was that the linear function $y = ax + b$ is used to separate the trend from oscillations because the power-law trend disappeared after HRF de-convolution (see Fig. 1).

Using Pearson's correlation, we evaluated the relationship between age and relative indices, including the mean and SD of GS, GS power at each frequency point, SCs of two oscillations, coefficients (a, b) of power-law and linear functions. Paired-samples t tests on SCs were performed to examine the effect of neurovascular coupling on the frequencies of two oscillations. Lastly, the correlation between the FD and age was calculated to evaluate the contribution of head motion to our results. Multiple comparisons were corrected with the false discovery rate (FDR) method ($q < 0.05$).

3 Results

There was no correlation between the mean of GS and age ($r = 0.04$, $p = 0.530$ for original data, $r = 0.06$, $p = 0.282$ for de-convolved data) because the residual of GS is close to 0 after noises regression. Negative correlations between the SD of GS and age, and between the range of GS power and age were found for original data ($r = -0.47$, $p < 0.001$; $r = -0.26$, $p < 0.001$), but the age effect was not significant for de-

convolved data (r = -0.06, p = 0.312; r = -0.11, p = 0.06), suggesting that the decline of GS variability with age is mainly contributed by neurovascular coupling.

The power of GS was significantly correlated with age in multiple frequency bands [0.007 ~ 0.01 Hz (r = 0.12 ~ 0.24), 0.013 ~ 0.022 Hz (r = -0.12~-0.20), 0.036 ~ 0.043 Hz (r = 0.12 ~ 0.13), 0.055 ~ 0.098 Hz (r = -0.12~-0.26), and 0.118 ~ 0.25 Hz (r = 0.12 ~ 0.32); FDR corrected, q < 0.05 corresponding r = ± 0.12] for the original data (Fig. 2A, left panel). After data de-convolution, significant positive and negative correlations (FDR corrected, q < 0.05 corresponding r = ± 0.14) were found at 0.037 ~ 0.05 Hz (frequency range with the lowest power; r = 0.14 ~ 0.17) and 0.067 ~ 0.112 Hz (frequency range with the highest power; r = -0.14~-0.26), respectively (Fig. 2B, left panel). A general trend was exhibited that lower power tends to increase with age while higher power tends to decrease with age.

The frequency range of oscillation 1 was 0.007 ~ 0.047 Hz and of oscillation 2 was 0.047 ~ 0.149 Hz for the original data. The SCs of the two oscillations tended to shift to higher frequencies with age (Fig. 2A, middle and right panels). For de-convolved data, oscillation 1 and oscillation 2 were located at 0.007 ~ 0.043 Hz and 0.043 ~ 0.195 Hz, respectively. Similar shifting to higher frequencies of their SCs was observed (Fig. 2B, middle and right panels). In addition, the SC of oscillation 1 was moved to lower frequencies (t = -43.3, p < 0.0001, Cohen's d = -2.42) whereas that of oscillation 2 was moved to higher frequencies (t = 46.0, p < 0.0001, Cohen's d = 2.56) by HRF de-convolution. These results suggested that oscillations shifting to higher frequencies is a general feature of brain aging, irrespective of the influence of neurovascular coupling on the middle frequency range.

The power-law trend of the original GS power spectrum was reduced with age (Fig. 3A, left panel), which was mainly determined by decreased coefficient *a* (the height of the power-law function; Fig. 3A, middle panel) rather than *b* (the curvature of the function; Fig. 3A, right panel), indicating that brain aging does not change the scale-free curve of GS power spectrum, but reduces the overall power especially in the lower frequency end. For the de-convolved data, the slope of linear trend (coefficient *a*) increased with age from negative to positive (Fig. 3B, left and middle panels), while the intercept (coefficient *b*) decreased with age (Fig. 3B, right panel), suggesting that the power of GS transfers from lower frequency to higher frequency as brain aging.

Finally, a significant positive correlation between the power of FD and age was found at 0.007 ~ 0.025 Hz. It was found both positive and negative and mainly negative correlation between the power of GS and age for the original data while no correlation for the de-convolved data within this frequency range, indicating that correlations between the power of GS and age are not determined by head motion.

4 Discussion

The current results revealed GS fluctuations varied as age in three aspects: general power reduction, power transferring to higher frequencies, and more even power distribution across frequencies, which indicate the correlation between GS fluctuations and age directly during the adult lifespan for the first time. More importantly, they argue a temporal dedifferentiation interpretation of brain aging. Age-related

variations of GS fluctuations have both neural and vascular origins. Elucidating the variation of GS fluctuations with age is essential to understand altered functional organization as brain aging.

To begin with, these findings are consistent with the general decline of local BOLD signal fluctuations as age in extensive regions [15,16], which suggested to represent a less complex neural system capable of smaller dynamic range, as well as an attenuated ability to efficiently process ever-changing external stimuli [32]. The present findings demonstrated that the GS, as an average of local signals, shows the same trend as local signals. Garrett and colleagues have demonstrated that local BOLD signal fluctuations are generally declined with age and predict age by more than four times over the mean BOLD signal [32]. The same trend also appeared from new born children to adults [33]. Combined with current findings, we suggest a general trend of low frequency power decline across human lifespan.

Secondly, frequencies of the two oscillations increased with age, as was showed in the first year of life [34]. But we do not know for sure if this trend persists throughout life for evidence of lifespan development is lacking. Furthermore, age-related frequency transfer was found in both power-law and linear trends. It is also known that frequency transfer occurred during the transition of the brain from resting-state to task-state, suggesting the brain expends more effort on immediate tasks [35]. These findings may indicate that low frequency brain organizations tend to run faster with age to maintain normal functions.

Thirdly, the GS power was more evenly distributed in aging brain, showing by (1) increased power with age at frequency bands with lower power and decreased power with age at frequency bands with higher power and (2) power transferring from lower frequencies with higher power to higher frequencies with lower power. These phenomena were much similar to the spatial dedifferentiation of brain aging, which argued that brain functions recruit more distributed rather than specialized brain regions in the elderly brain [36]. Analogously, we interpret the more evenly distributed power in elderly brain as temporal dedifferentiation. The spatiotemporal dedifferentiation may be of importance for preserving brain functions and preventing functional degeneration during brain aging [37].

Finally, we demonstrated that the decline and temporal dedifferentiation of GS fluctuations with age are primarily contributed by neural activity, less contributed by vascular factors, and almost unaffected by head motion. Grinband et al. suggested that neurovascular coupling does not change significantly with normal aging [38], whereas Tsvetanov et al. argued that the age effect of BOLD signal variability is explained by cardiovascular and cerebrovascular factors [14]. Chen et al. further demonstrated that resting-state networks formed by so-called physiological noises are highly overlapping with intrinsic networks [39]. Considering that the GS contains both neural information and non-neural noises while these noises such as head motion [40], respiratory [41], and cardiac signals [42] have been demonstrated to contain meaningful physiological and pathological information, it is necessary to isolate different contributions of these components to brain aging.

Some limitations remain. First, the age effect of physiological noises was indirectly tested due to the lack of such information in the open database. The actual contributions of different components (i.e.

respiratory and cardiac signals) should be tested directly in future studies. Second, head motion parameters were strictly restricted and regressed out, which may eliminate motion-related physiological activities [40]. Thus, the contribution of head motion to brain aging warrants further studies. Third, the cognitive relevance of our results cannot be determined because there is no cognitive measurement in this dataset. Given the close relationship between brain signal fluctuations and cognition in particular frequency bands [16], our findings in multiple frequency bands may be associated with various cognitions which deserves in-depth studies. Finally, there were more females (n = 194) than males (n = 128) in the final analysis. We regressed out sex information and did not test the sex effect because it was outside the scope of this study. However, the influence of sex on brain aging is inconclusive and deserves further investigations [43].

5 Conclusion

We investigated GS fluctuations across the adult lifespan. The decline and temporal dedifferentiation of GS power with age were confirmed to be general patterns of brain aging. These patterns may be driven by various physiological and psychological components. The temporal dedifferentiation extends the classical theory of spatial dedifferentiation in aging brain and requires further verification.

Declarations

Author contributions

Y.W. designed the study. Y.W., Y.A., and X.C. analyzed the data. Y.W., Y.A., X.C., and J.K. wrote the manuscript. All authors reviewed and edited the manuscript. All authors read and approved the manuscript.

References

1. Ferreira, L. K. & Busatto, G. F. Resting-state functional connectivity in normal brain aging. *Neuroscience and Biobehavioral Reviews*, **37**, 384–400 (2013).
2. Vij, S. G., Nomi, J. S., Dajania, D. R. & Uddin, L. Q. Evolution of spatial and temporal features of functional brain networks across the lifespan., **173**, 498–508 (2018).
3. Murphy, K. & Fox, M. D. Towards a consensus regarding global signal regression for resting state functional connectivity MRI., **154**, 169–173 (2017).
4. Scalabrini, A. *et al.* All roads lead to the default-mode network—global source of DMN abnormalities in major depressive disorder. *Neuropsychopharmacology*, **45**, 2058–2069 (2020).
5. Fox, M. D., Zhang, D., Snyder, A. Z. & Raichle, M. E. The global signal and observed anticorrelated resting state brain networks. *Journal of Neurophysiology*, **101**, 3270–3283 (2009).
6. Power, J. D., Plitt, M., Laumann, T. O. & Martin, A. Sources and implications of whole-brain fMRI signals in humans., **146**, 609–625 (2017).

7. Wong, C. W., Olafsson, V., Tal, O. & Liu, T. T. The amplitude of the resting-state fMRI global signal is related to EEG vigilance measures., **83**, 983–990 (2013).
8. Li, J. *et al.* Topography and behavioral relevance of the global signal in the human brain. *Sci. Rep*, **9**, 14286 (2019).
9. Gutierrez-Barragan, D., Basson, M. A., Panzeri, S. & Gozzi, A. Infraslow state fluctuations govern spontaneous fMRI network dynamics. *Curr. Biol*, **29**, 2295–2306 (2019).
10. Yang, G. J. *et al.* Altered global brain signal in schizophrenia. *Proceedings of the National Academy of Sciences of the United States of America*, **111**, 7438–7443 (2014).
11. Ao, Y., Ouyang, Y., Yang, C. & Wang, Y. Global signal topography of the human brain: A novel framework of functional connectivity for psychological and pathological investigations. *Frontiers in Human Neuroscience*, **15**, 644892 (2021).
12. Huang, X., Long, Z. & Lei, X. Electrophysiological signatures of the resting-state fMRI global signal: A simultaneous EEG-fMRI study. *Journal of Neuroscience Methods*, **311**, 351–359 (2019).
13. Turchi, J. *et al.* The basal forebrain regulates global resting-state fMRI fluctuations., **97**, 940–952 (2018).
14. Tsvetanov, K. A. *et al.* The effects of age on resting-state BOLD signal variability is explained by cardiovascular and cerebrovascular factors., **58**, e13714 (2021).
15. Nomi, J. S., Bolt, T. S., Ezie, C., Uddin, L. Q. & Heller, A. S. Moment-to-moment BOLD signal variability reflects regional changes in neural flexibility across the lifespan. *The Journal of Neuroscience*, **37**, 5539–5548 (2017).
16. Yang, A. C., Tsai, S. J., Lin, C. P., Peng, C. K. & Huang, N. E. Frequency and amplitude modulation of resting-state fMRI signals and their functional relevance in normal aging. *Neurobiology of Aging*, **70**, 59–69 (2018).
17. Wei, D. *et al.* Structural and functional brain scans from the cross-sectional Southwest University adult lifespan Dataset. *Scientific Data*, **5**, 180134 (2018).
18. Yan, C. G. & Zang, Y. F. DPARSF: a MATLAB toolbox for “pipeline” data analysis of resting-state fMRI. *Frontiers in Systems Neuroscience*, **4**, 1–7 (2010).
19. Wang, X. *et al.* Altered dynamic global signal topography in antipsychotic-naive adolescents with early-onset schizophrenia. *Schizophr. Res*, **208**, 308–316 (2019).
20. Yan, C. G. *et al.* A comprehensive assessment of regional variation in the impact of head micromovements on functional connectomics. *NeuroImage*, **76**, 183–201 (2013).
21. Tzourio-Mazoyer, N. *et al.* Automated anatomical labeling of activations in SPM using a macroscopic anatomical parcellation of the MNI MRI single-subject brain. *NeuroImage*, **15**, 273–289 (2002).
22. Wang, Y. F. *et al.* Steady-state BOLD response to higher-order cognition modulates low frequency neural oscillations. *Journal of Cognitive Neuroscience*, **27**, 2406–2415 (2015).

23. Baria, A. T., Baliki, M. N., Parrish, T. & Apkarian, A. V. Anatomical and functional assemblies of brain BOLD oscillations. *Journal of Neuroscience*, **31**, 7910–7919 (2011).
24. Liu, F. *et al.* Dynamic functional network connectivity in idiopathic generalized epilepsy with generalized tonic–clonic seizure. *Hum. Brain. Mapp*, **38**, 957–973 (2017).
25. Wen, H. & Liu, Z. Broadband electrophysiological dynamics contribute to global resting-state fMRI signal. *Journal of Neuroscience*, **36**, 6030–6040 (2016).
26. Ries, A. *et al.* Grading of frequency spectral centroid across resting-state networks. *Frontiers in Human Neuroscience*, **12**, 436 (2018).
27. Friston, K. J. *et al.* Statistical parametric maps in functional imaging: a general linear approach. *Hum. Brain. Mapp*, **2**, 189–210 (1994).
28. Wang, Y. F. *et al.* Steady-state BOLD response modulates low frequency neural oscillations. *Sci. Rep*, **4**, 7376 (2014).
29. Tagliazucchi, E., Balenzuela, P., Fraiman, D. & Chialvo, D. R. Criticality in large-scale brain fMRI dynamics unveiled by a novel point process analysis. *Frontiers in Physiology*, **3**, 15 (2012).
30. Wu, G. R., Stramaglia, S., Chen, H., Liao, W. & Marinazzo, D. Mapping the voxel-wise effective connectome in resting state fMRI. *PLoS ONE*, **8**, e73670 (2013).
31. Wu, G. R. *et al.* A blind deconvolution approach to recover effective connectivity brain networks from resting state fMRI data. *Med. Image. Anal*, **17**, 365–374 (2013).
32. Garrett, D. D., Kovacevic, N., McIntosh, A. R. & Grady, C. L. Blood oxygen level-dependent signal variability is more than just noise. *The Journal of Neuroscience*, **30**, 4914–4921 (2010).
33. Fransson, P. *et al.* Early development of spatial patterns of power-law frequency scaling in fMRI resting-state and EEG data in the newborn brain. *Cereb. Cortex*, **23**, 638–646 (2013).
34. Alcauter, S. *et al.* Frequency of spontaneous BOLD signal shifts during infancy and correlates with cognitive performance. *Dev. Cogn. Neurosci*, **12**, 40–50 (2015).
35. He, B. J., Zempel, J. M., Snyder, A. Z. & Raichle, M. E. The temporal structures and functional significance of scale-free brain activity., **66**, 353–369 (2010).
36. Natasha, R. M. & Mark, D. E. Region-specific changes in prefrontal function with age: a review of PET and fMRI studies on working and episodic memory., **128**, 1964–1983 (2005).
37. Sala-Llonch, R., Bartrés-Faz, D. & Junque, C. Reorganization of brain networks in aging: A review of functional connectivity studies. *Frontiers in Psychology*, **6**, 663 (2015).
38. Grinband, J., Steffener, J., Razlighi, Q. R. & Stern, Y. BOLD neurovascular coupling does not change significantly with normal aging. *Hum. Brain. Mapp*, **38**, 3538–3551 (2017).
39. Chen, J. E. *et al.* Resting-state “physiological networks”. *NeuroImage*, **213**, 116707 (2020).
40. Zeng, L. L. *et al.* Neurobiological basis of head motion in brain imaging. *Proceedings of the National Academy of Sciences of the United States of America*, **111**, 6058–6062 (2014).
41. Park, H. D. *et al.* Breathing is coupled with voluntary action and the cortical readiness potential. *Nature Communications*, **11**, 289 (2020).

42. Mosher, C. P. *et al.* Cellular classes in the human brain revealed in vivo by heartbeat-related modulation of the extracellular action potential waveform. *Cell Reports*, **30**, 3536–3551 (2020).

43. Joel, D. Beyond the binary: Rethinking sex and the brain. *Neuroscience & Biobehavioral Reviews*, **122**, 165–175 (2021).

Figures

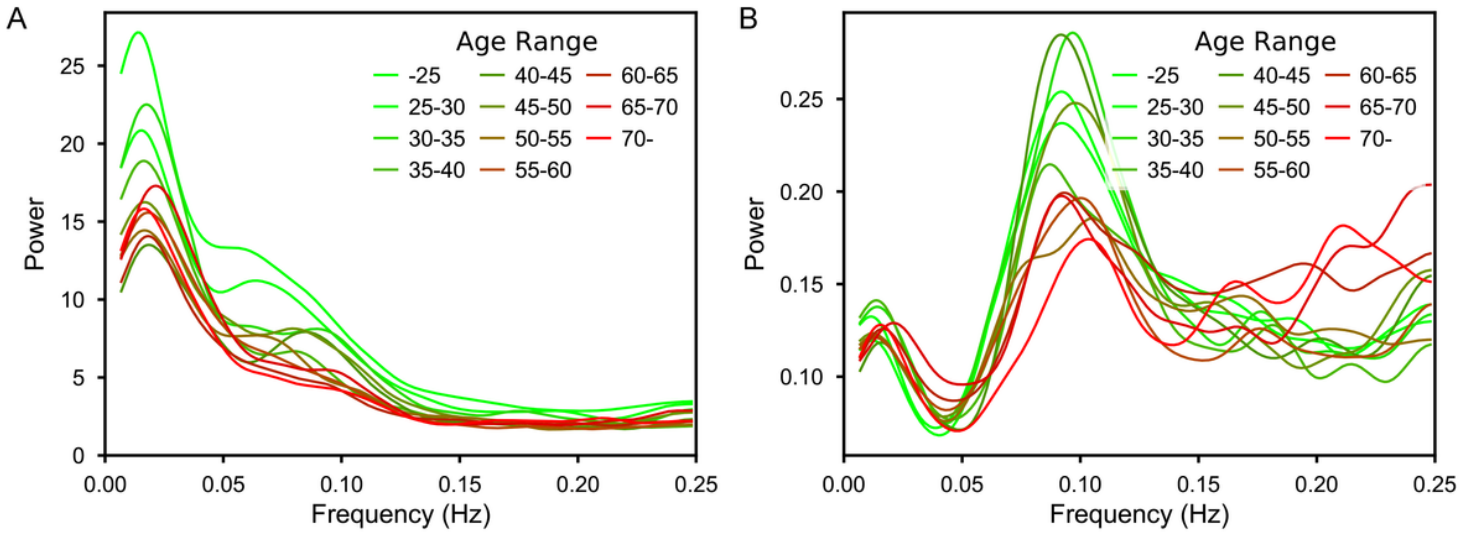

Figure 1

The power spectra of GS for original data (A) and de-convolved data (B), showing in multiple age ranges.

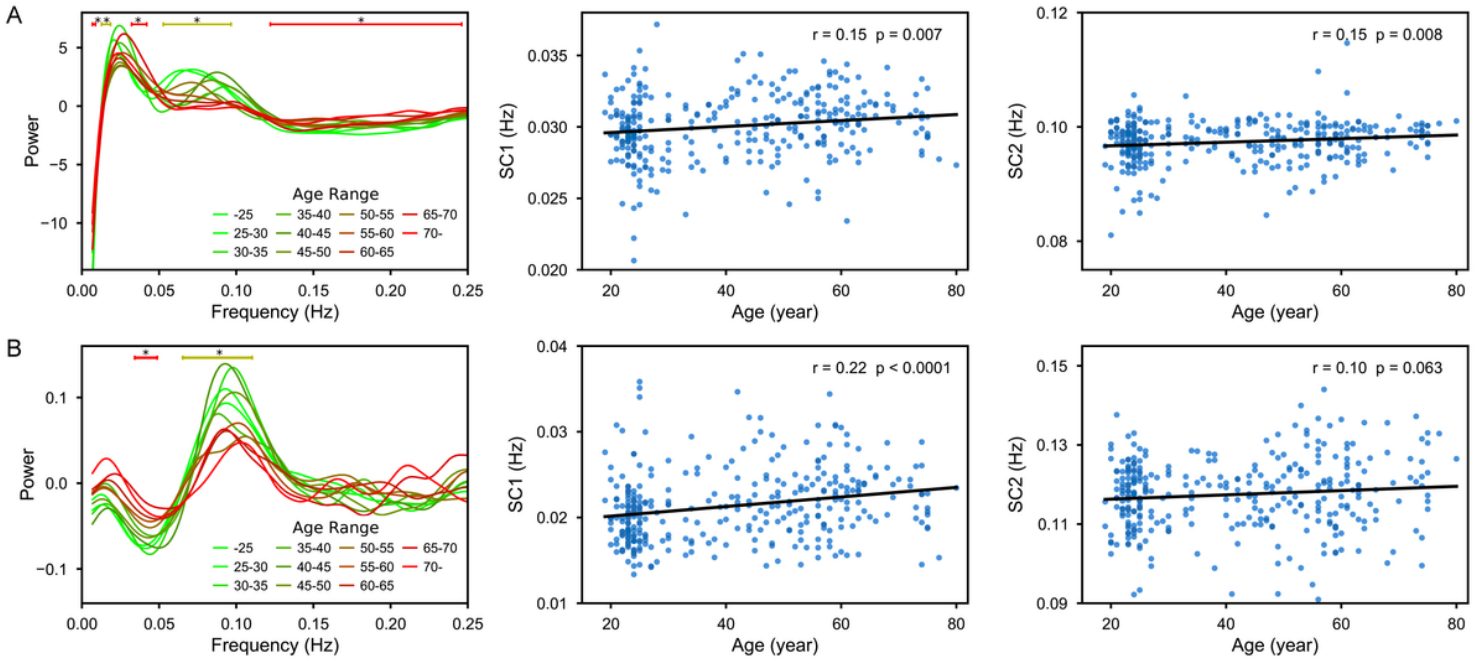

Figure 2

The variation of GS power with age for original data (A) and de-convolved data (B). Left panel: the power spectra of GS after detrending. * with black segment represents positive correlation between age and power; * with gray segment represents negative correlation between age and power. Middle panel: correlation between the SC of oscillation 1 and age. Right panel: correlation between the SC of oscillation 2 and age.

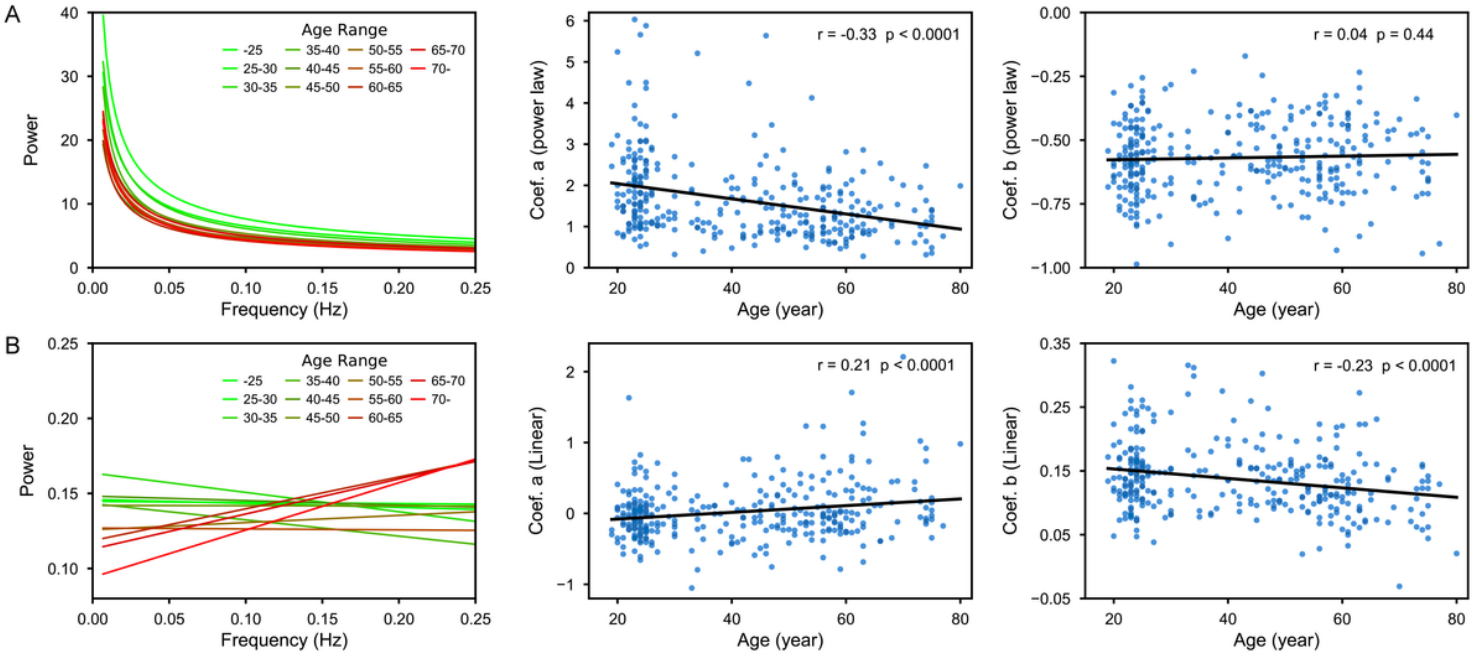

Figure 3

The relationship between age and the power-law trend of the power spectrum of GS for the original data (A) and the linear trend for the de-convolved data (B). Left panel: trends of the power spectra of GS. Middle panel: correlation between the coefficient a of trend functions and age. Right panel: correlation between the coefficient b of trend functions and age.